Performance and design of an off-resonant continuous-wave Raman laser

K. S. Repasky, J. K. Brasseur, L. Meng, and J. L. Carlsten

Department of Physics, Montana State University, Bozeman, Montana 59717

Received December 23, 1997; revised manuscript received March 3, 1998

A steady-state theory that describes the performance of a cw off-resonant Raman laser is presented. The cw Raman laser is constructed in a nonconfocal high-finesse cavity that allows for high Raman gain with low pump powers. Threshold values of the pump laser used to pump the cw Raman laser are predicted to be as low as 1 mW. The maximum photon-conversion efficiency for the cw Raman laser is predicted to be 50%. The theory is compared with experimental results from a cw Raman laser that operates with a pump wavelength of 532 nm and a Stokes-shifted wavelength of 683 nm. A threshold pump power of 2 mW and a maximum photon-conversion efficiency of 34% ± 6% was measured. With the mirrors used in the experiment, these values correspond to the predictions from the steady-state cw Raman laser theory. The theoretical model is then used to design cw Raman lasers operate near the maximum conversion efficiency in the 1–4-μm wavelength region. [S0740-3224(98)01106-0]

OCIS codes: 140.3550, 190.5650, 290.5860, 140.3070, 140.3480, 140.4780.

1. INTRODUCTION

With the recent advancements in mirror technology, highly reflective mirrors coated for multiple wavelengths with low absorption losses are now commercially available. These mirrors are currently used in high-finesse cavities[1,2] (HFC's) that have finesses of 10,000–50,000. The power inside an HFC scales approximately as the input power multiplied by the finesse.[3] For example, an interferometer with a finesse of 50,000 and an input power of 20 mW will have a power of 1 kW inside the cavity. The high power inside the HFC makes it possible to exploit nonlinear processes, such as Raman scattering, with low-power cw lasers, such as diode lasers.

Raman scattering[4–7] is an inelastic scattering process in which a pump photon scatters off a molecule. Some of the energy of the pump photon is left with the molecule, causing the molecule to vibrate or rotate. The scattered photon is less energetic than the pump photon and thus has a longer wavelength. Raman lasers[8] use this inelastic scattering process to create Stokes-shifted outputs. However, because of the high pump powers needed to generate the Raman gain for the off-resonant Raman scattering, pulsed lasers have typically been used to pump the Raman medium.[9,10]

Although cw Raman lasers have been built to operate near a molecular or atomic resonance[11–14] where the Raman gain is large, these lasers are tunable only over a narrow region near the molecular or atomic resonance. Furthermore, the pump wavelength needed for these cw Raman lasers is dictated by the energy-level structure of the molecule or atom.

Building a cw Raman laser in a HFC allows one to pump a Raman system far off the molecular or atomic resonance, because the high pump powers inside the HFC that result from the highly reflective mirrors translate to large Raman gains. A cw Raman laser that is built far off the molecular or atomic resonance has advantages over the cw Raman laser built near a molecular or atomic resonance. These advantages include a large range of pump wavelengths that can drive the Raman laser, which corresponds to a large tuning range.

With room-temperature diodes, Raman scattering in a HFC can be used to create lasers in the hard-to-reach 1–4-μm wavelength region of the spectrum. Figure 1 shows the available room-temperature diode lasers and the Raman-shifted wavelengths that these lasers can reach in various Raman active media. These cw Raman lasers can find immediate applications in spectroscopy because many atmospheric molecules[15–17] and pollutants[17,18] have strong absorptions in the 1–4-μm wavelength region of the spectrum.

In this paper a steady-state theory is presented that describes the output Stokes power as a function of the input pump power for a cw Raman laser built in a nonconfocal HFC. This theory models the performance of the cw Raman laser, including the threshold condition and the Stokes power-conversion efficiency. From this theory a relatively simple method for designing a cw Raman laser that operates near the maximum conversion efficiency is presented.

Experimental results from a cw Raman laser are presented. The output Stokes power was measured as a function of the input pump power and is compared with that predicted by the steady-state theory. The experimental results compare favorably with the predictions from the theory presented in this paper.

The paper is organized as follows. In Section 2 we present the details of the theory used to describe a cw Raman laser built in a HFC. In Section 3 we examine the output Stokes power and the reflected and the transmitted pump powers as functions of the input pump power as well as the threshold condition. In Section 4 the conversion efficiency for the cw Raman laser is studied. In Section 5 the theoretical model is compared with the experi-

0740-3224/98/061667-07$15.00

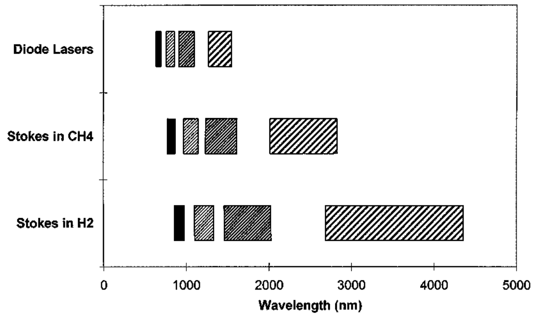

Fig. 1. Wavelengths for the available room-temperature laser diodes and the wavelengths these diodes can be shifted to by use of Raman scattering in different Raman media. By use of the available room-temperature diode lasers as pump sources, cw Raman lasers can be built to cover the 1–4-μm spectral region.

mental performance of a cw Raman laser. In Section 6 we present a simple procedure for designing cw Raman lasers that perform at or near the maximum conversion efficiency. Finally, in Section 7, some concluding remarks are made.

2. THEORY

The cw Raman laser consists of an HFC filled with a Raman active medium, such as H_2. The HFC has two highly reflective mirrors ($R > 99.98\%$) with low absorption loss [$A < 15$ parts per million (ppm)] and is set up in a nonconfocal cavity configuration with a mirror separation distance l, which is smaller than the radius of curvature of the mirrors, R_m. In this section a steady-state theory that describes the output Stokes power as a function of the input pump power for a cw Raman laser is developed.

The Stokes field is written as[19]

$$E_S(z,\ t) = {}^1\!/_2\ E_S(t)\exp(-i\omega_S t)u(z) + \text{c.c.}, \qquad (1)$$

where c.c. stands for the complex conjugate and $E_S(t)$ is the slowly varying envelope of the Stokes field, is a complex function of time, and includes the phase information. Here ω_S is the frequency of the Stokes field, and $u(z)$ contains the spatial information and is written as[19]

$$u(z) = \sin(kz), \qquad (2)$$

where

$$kc = \frac{N\pi c}{l} = \Omega, \qquad (3)$$

where c is the speed of light, Ω is the resonant frequency of the HFC cavity that is close to but not necessarily equal to the Stokes frequency ω_S, and N is an integer. The polarization at the Stokes frequency is written in a similar manner as[19]

$$\wp_S(z,\ t) = {}^1\!/_2\wp_S(t)\exp(-i\omega_S t)u(z) + \text{c.c.}, \qquad (4)$$

where $\wp_S(t)$ is the complex slowly varying envelope of the polarization.

The wave equation that describes the growth of the slowly varying Stokes field $E_S(t)$ is[19]

$$\frac{\partial E_S(t)}{\partial t} = -i(\Omega - \omega_S)E_S(t) + \frac{1}{2}\,i\,\frac{\omega_S}{\epsilon}\,\wp_S(t), \qquad (5)$$

where ϵ is the dielectric permeability of the Raman active medium. To understand the Raman gain, we next develop an expression for $\wp_S(t)$, the slowly varying envelope of the polarization that oscillates near the Stokes frequency.

The polarization can be written as[19]

$$\wp_S(t) = 2\exp(i\omega_S t)\,\frac{1}{M}\int_0^l u^*(z)\mathrm{Tr}(\rho p)\mathrm{d}z, \qquad (6)$$

where $M = \int_0^l |u(z)|^2 \mathrm{d}z$ and is a normalization factor, ρ is the density matrix, and p is the polarization matrix where the p_{mn} element of the matrix is $p_{mn} = ex_{mn} = e\langle m|x|n\rangle$. Here e is the electronic charge and $\mathrm{Tr}(\rho p)$ stands for the trace of the matrix product of the density matrix and polarization matrix.

The Raman system for H_2 is a three level system with level $|1\rangle$ the ground state, level $|2\rangle$ the first excited electronic state, and level $|3\rangle$ the first excited vibrational level. The trace of the product of the density matrix and the polarization matrix is given by

$$\mathrm{Tr}(\rho p) = e(x_{21}\rho_{12} + x_{21}^*\rho_{21} + x_{23}^*\rho_{23} + x_{23}\rho_{32}). \qquad (7)$$

In Eq. (7), only the ρ_{23} term will oscillate such that $\wp_S(t)$ is slowly varying. Assuming that the HFC is on resonance so that $\Omega = \omega_S$ and using the equations for the density-matrix elements, one can use Eqs. (5–7) to obtain

$$\frac{\partial E_S(t)}{\partial t} = G_S|E_p(t)|^2 E_S(t), \qquad (8)$$

where G_S represents the gain at the Stokes frequency and depends on the medium's parameters. One can write Eq. (8) in terms of the Stokes power by multiplying by $E_S^*(t)$ and noting that $|E_S(t)|^2$ is proportional to the Stokes power. The result is

$$\frac{\partial \Pi_S}{\partial t} = 2G_S\Pi_p\Pi_S - L_S\Pi_S, \qquad (9)$$

where $\Pi_S(\Pi_p)$ is the Stokes (pump) power inside the HFC and L_S is phenomenologically added to account for losses of the Stokes power that are due to transmission through the mirrors.

The gain (G_S) can be found when we compare Eq. (9) with Ref. 20 (with $L_S = 0$). The result is that

$$G_S = \frac{c}{2l}\left[\frac{4\alpha_g \tan^{-1}(l/b)}{\lambda_S + \lambda_p}\right], \qquad (10)$$

where α_g is the plane-wave gain coefficient,[21,22] $b = [l(2R_m - l)]^{1/2}$ is the confocal parameter of the HFC, and $\lambda_S(\lambda_p)$ is the Stokes (pump) wavelength.

We can also find an expression for the loss term by setting the gain in Eq. (9) to zero. The Stokes power is then

$$\Pi_S = \Pi_S(0)\exp(-L_S t). \qquad (11)$$

But since this is the power inside the HFC, $\Pi_S = R\Pi_S(0)$ after a single pass that occurs in a time $t = l/c$. Thus the loss L_S is

$$L_S = -(c/l)\ln(R). \qquad (12)$$

In the steady-state limit, $\partial \Pi_S / \partial t = 0$, and this allows us to write a condition for the pump power inside the HFC, Π_p, as

$$\Pi_p = \frac{L_S l(\lambda_S + \lambda_p)}{4c\alpha_g \tan^{-1}(l/b)}. \tag{13}$$

Now consider the picture for the HFC shown in Fig. (2). The incident pump field is E_0, r is the field reflectivity of the mirrors, t is the field transmission of the mirrors, and d is the field depletion factor that accounts for the conversion of the pump field to the Stokes field inside the HFC. The depletion factor can range between 0 and 1.

Summing the pump field inside the HFC and squaring this sum leads to a result for the pump power inside the HFC. This result is

$$\Pi_p = P_0 \frac{d^2 T}{(1 - \sqrt{R})^2}, \tag{14}$$

where P_0 is the input pump power, $T = t^2$ is the transmission of the mirrors, and $R = r^2$ is the reflectivity of the mirrors. In the steady-state approximation, the pump field reaches its steady-state value, and this is then converted to a Stokes field so that d is included only once per pass in this model. From Eqs. (13) and (14), a condition which describes the depletion factor is reached:

$$d^2 = \frac{L_S}{2G_S} \frac{(1 - \sqrt{R})^2}{T} \frac{1}{P_0}. \tag{15}$$

If d as calculated from Eq. (15) is larger than 1, then the Stokes losses are greater than the Stokes gain, and no conversion to Stokes will occur. In this case d is set to its upper limit of 1.

We can find the transmitted and the reflected pump powers by summing the reflected and the transmitted fields in Fig. (2). This leads to the total pump power outside the HFC, P_p, and is

$$P_p = P_0\left[R\left(\frac{dT}{1 - R} - 1\right)^2 + \left(\frac{dT}{1 - R}\right)^2\right], \tag{16}$$

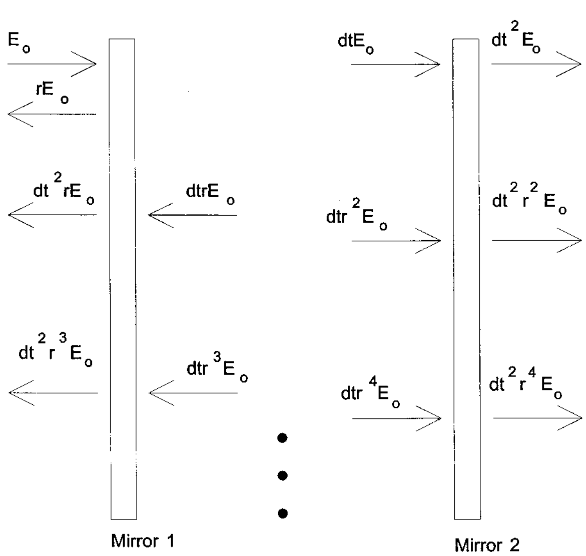

Fig. 2. Schematic diagram of fields reflected from, and transmitted through and between, the mirrors of the HFC.

where the first term on the right-hand side of Eq. (16) is the reflected pump power, while the second term is the transmitted pump power.

We can also find the absorption of the pump power at the two mirrors by summing the fields at each mirror, squaring to get the power, and multiplying by the mirror absorption A. The absorption of the pump power by the mirrors, Δ, is

$$\Delta = AP_0\left[1 + \frac{d^2 TR}{(1 - R)^2} + \frac{d^2 T}{(1 - R)^2}\right]. \tag{17}$$

The output Stokes power can now be found from energy conservation. The input pump power is P_0, while the unconverted pump power outside the HFC is P_p. The amount of pump power lost to absorption is Δ. So the total converted Stokes power is

$$P_S = (\lambda_p/\lambda_S)(P_0 - P_p - \Delta), \tag{18}$$

where the ratio of the wavelengths is used to scale the power at the pump wavelength to that at the Stokes wavelength.

3. THRESHOLD AND OUTPUT POWERS

The Raman medium used for the calculations in this section and for the rest of the paper is H_2, which has a Raman shift[23] of 4155 cm^{-1}. Unless otherwise stated, the cavity length is $l = 3$ cm and the mirror radius of curvature is $R_m = 100$ cm. The Raman plane-wave gain coefficient[21,22] for a pump wavelength of $\lambda_p = 532$ nm (795 nm, 1330 nm, 1550 nm) is $\alpha_g = 2.5 \times 10^{-9}$ cm/W (1.4×10^{-9} cm/W, 0.53×10^{-9} cm/W, 0.36×10^{-9} cm/W).

The depletion factor d accounts for the amount of conversion of pump power to Stokes power inside the HFC and is defined by Eq. (15). The depletion factor ranges from 1 to 0, with $d = 1$ corresponding to no Stokes conversion and $d = 0$ corresponding to maximum Stokes conversion inside the HFC. When Eq. (15) is greater than 1, the losses of the HFC at the Stokes wavelength are greater than the Stokes gain, and the cw Raman laser is below threshold. In this case, d is set to its upper limit of 1. The threshold condition for a cw Raman laser is thus

$$P_0(\text{th}) = \frac{L_S}{2G_S} \frac{(1 - \sqrt{R})^2}{T}, \tag{19}$$

where $P_0(\text{th})$ is the minimum input pump power that is required for the Stokes conversion to start for the cw Raman laser.

Figure 3 shows the output Stokes power as a function of input pump power for four different pump wavelengths. The pump wavelengths are 532 nm, which corresponds to a frequency-doubled Nd:YAG laser; 795 nm, which corresponds to diode lasers and Ti:Sapphire lasers; and 1330 and 1550 nm, which correspond to diode lasers used in telecommunications. The mirror reflectivities used in the calculations are $R = 99.98\%$, and the mirror absorp-

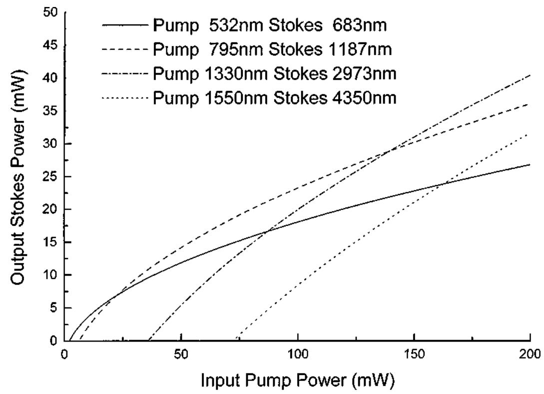

Fig. 3. Plot of the output Stokes power as a function of the input pump power. Solid, dashed, dotted–dashed, and dotted curves denote pump lasers at 532, 795, 1330, and 1550 nm, respectively, and Stokes-shifted wavelengths of 683, 1187, 2973, and 4350 nm, respectively. The mirror reflectivities at both the pump and the Stokes wavelengths are 99.98%, and the mirror absorptions at both the pump and the Stokes wavelengths are 15 ppm.

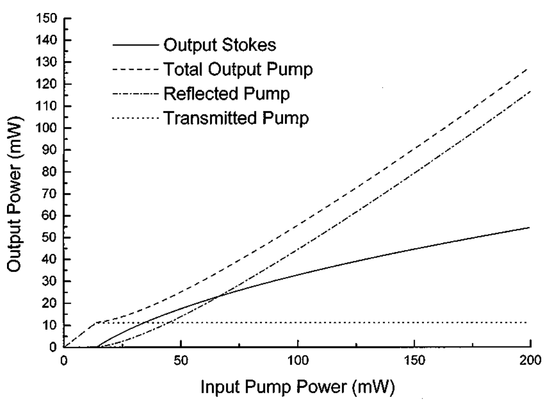

Fig. 4. Plot of the Stokes output power (solid curve), the total output pump power (dashed curve), the reflected pump power (dotted–dashed curve) and the transmitted pump power (dotted curve) for a pump wavelength of 532 nm and a Stokes-shifted wavelength of 683 nm. The mirror reflectivities at both the pump and the Stokes wavelengths are $R = 99.95\%$, and the mirror absorptions at both the pump and the Stokes wavelengths are $A = 50$ ppm.

tions are $A = 15$ ppm at both the pump and the Stokes wavelengths. The effects of mirror reflectivity and absorption are studied below. Mirrors with these reflectivities and absorptions are commercially available.[24] Thresholds range from 3 mW for a pump wavelength of 532 nm to a threshold of 72 mW for a pump wavelength of 1550 nm. One can reduce the threshold for the longer-wavelength pump lasers by increasing the cavity length of the HFC and thus increasing the gain.

Note in Fig. 3 that the output power levels off more rapidly for shorter wavelengths. At first glance this may seem surprising, but it is related to the maximum conversion efficiency being dependent on the gain. For shorter wavelengths the gain is higher, which leads to a lower threshold and a lower-input pump power for maximum conversion efficiency. In Section 4 we present plots of conversion efficiency versus pump power for various reflectivities that show similar crossings (see Fig. 5 below, for example).

Figure 4 is a plot of the output Stokes power (solid curve), the total output pump power (dashed curve), the transmitted pump power (dotted curve), and the reflected pump power (dotted–dashed curve) for a Raman laser with a pump wavelength of 532 nm and a Stokes-shifted wavelength of 683 nm as a function of the input pump power. To show the threshold condition more clearly, we set the mirror reflectivities at both the pump and the Stokes wavelengths were set to $R = 99.95\%$, and the mirror absorptions at both the pump and the Stokes wavelengths were set to $A = 50$ ppm. The threshold for the input pump power to start converting to Stokes power for this case is 15 mW. Below this threshold, the transmitted pump grows linearly with a slope of less than 1, because the mirror has some absorption. Above the threshold the transmitted pump power remains at a constant power. The reflected pump power below threshold is small but not zero. The reason the reflected pump power is not zero below the threshold value is that the mirror absorption caused the initial reflected pump beam not to be canceled by the subsequent pump beam that is leaked out of the cavity. The Stokes power grows above threshold when the pump power is converted inside the HFC. However, as the pump power is converted to Stokes power, the cancellation of the initially reflected pump beam by the cavity leakage is not complete. This is the reason that the reflected pump beam grows as the cavity is pumped harder. The ratio of output Stokes power to input pump power at an input pump power of 50 mW is 38%, while at 200 mW this ratio is 27%. The ratio of the reflected pump power to input pump power at an input pump power of 50 mW is 34%, while at an input pump power of 200 mW this ratio is 65%. We must carefully consider the design parameters when building a cw Raman laser so that the ratio of the output Stokes power to the input pump power is maximized while the ratio of the reflected pump power to the input pump power is minimized. This is discussed further in Sections 4 and 6.

4. CONVERSION EFFICIENCY

The Stokes power-conversion efficiency for the Raman laser is defined as the ratio of the Stokes output power to the input pump power. The Stokes power conversion efficiency, C_S, can be written from Eqs. (16)–(18) as

$$C_S = \frac{\lambda_p}{\lambda_S}\left\{T + d\,\frac{2TR}{1-R} - d^2(1+R)\left[\frac{T^2 + AT}{(1-R)^2}\right]\right\}. \tag{20}$$

The Stokes power-conversion efficiency is a function of the depletion factor and hence a function of the input pump power. The Stokes photon-conversion efficiency, C_{ph}, which relates the number of output Stokes photons to the number of input pump photons, is related to the Stokes power-conversion efficiency by the relationship

$$C_{\mathrm{ph}} = \frac{\lambda_S}{\lambda_p}\,C_S\,. \tag{21}$$

Figure 5 is a plot of the Stokes photon-conversion efficiency as a function of the input pump power. The mirror absorptions at both the pump and the Stokes wave-

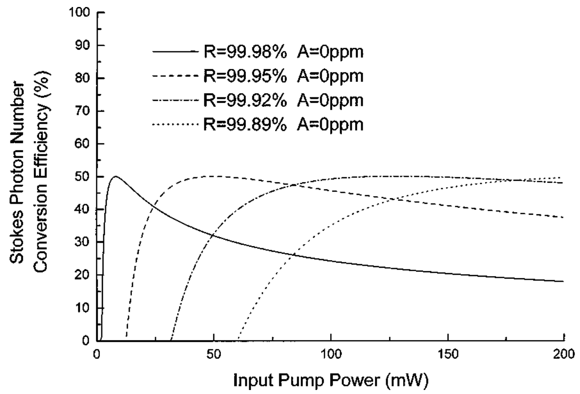

Fig. 5. Plot of the Stokes photon-conversion efficiency as a function of input pump power. The pump (Stokes) wavelength is 532 nm (683 nm). The mirror absorptions at both the pump and the Stokes wavelengths are $A = 0$ ppm. The solid, dashed, dotted–dashed, and dotted curves were calculated, respectively, for mirror reflectivities of $R = 99.98\%$, 99.95%, 99.92%, and 99.89%. The maximum photon-conversion efficiency for each mirror reflectivity is 50%.

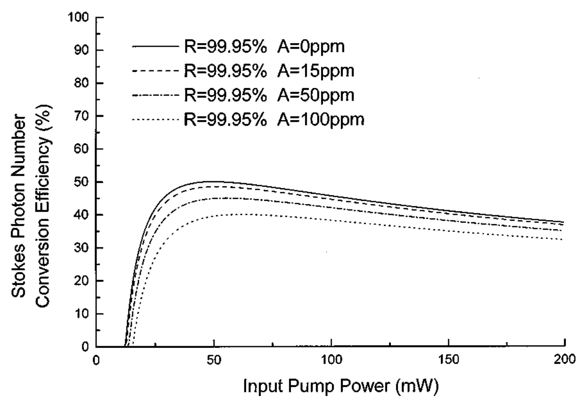

Fig. 6. Plot of the Stokes photon-conversion efficiency as a function of the input pump power. The pump (Stokes) wavelength is 532 nm (683 nm). The mirror reflectivities at both the pump and the Stokes wavelengths are $R = 99.95\%$. The solid dashed, dotted–dashed, and dotted curves were calculated, respectively, for mirror absorptions of $A = 0$, 15, 50, and 100 ppm.

lengths are set to zero, and the mirror reflectivities at both the pump and the Stokes wavelengths range from 99.89% to 99.98%. The threshold for the Stokes conversion increases as the mirror reflectivity decreases. The conversion efficiency for each of the four mirror reflectivities reaches a peak value of $C_{\mathrm{ph}}(\max) = 50\%$ and then falls from its peak value as the input pump is increased. Choosing the proper mirror reflectivities for a given input pump power is imperative to designing an efficient cw Raman laser. For instance, if an input pump power of 40 mW is being used to pump the Raman laser, then the most efficient cw Raman laser will be built with mirror reflectivities at $R = 99.95\%$.

Figure 6 is a plot of the Stokes photon-conversion efficiency as a function of the input pump power for various mirror absorptions. The mirror reflectivities at both the pump and the Stokes wavelengths are set at $R = 99.95\%$, and the mirror absorptions range from 0 to 100 ppm. The higher the absorption, the larger the threshold value for the Raman conversion. Also, larger absorptions result in lower peak-conversion efficiencies. Low-loss mirrors are commercially available with losses that are due to absorption as low as 15 ppm.[24]

5. EXPERIMENTAL DESCRIPTION AND RESULTS

The experimental setup used to measure the output Stokes power as a function of the input pump power is similar to the experimental setup described in Ref. 25. The pump laser wavelength is 532 nm. The Raman medium used in this experiment is H_2 at a pressure of 10 atm, and the Raman plane-wave gain coefficient is $\alpha_g = 2.5 \times 10^{-9}$ cm/W. H_2 has a Raman shift of 4155 cm^{-1}, thus making the Raman-shifted Stokes wavelength 683 nm. The mirror reflectivity at the pump (Stokes) wavelength is $R = 99.984\%$ ($R = 99.984\%$), and the mirror absorption at the pump (Stokes) wavelength is $A = 78$ ppm ($A = 78$ ppm). The radius of curvature of the mirrors is $R_m = 50$ cm, and the cavity length is $l = 7.3$ cm.

Figure 7 is a plot of the output Stokes power as a function of the input pump power. The filled circles are the experimental measurements, and the solid curve is the

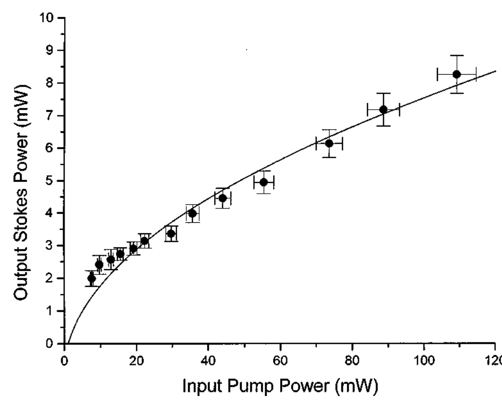

Fig. 7. Plot of the output Stokes power at 683 nm as a function of the input pump power at 532 nm. Solid curve, the theoretical predictions; filled circles, experimental measurements. The experiment and the theory are in good agreement.

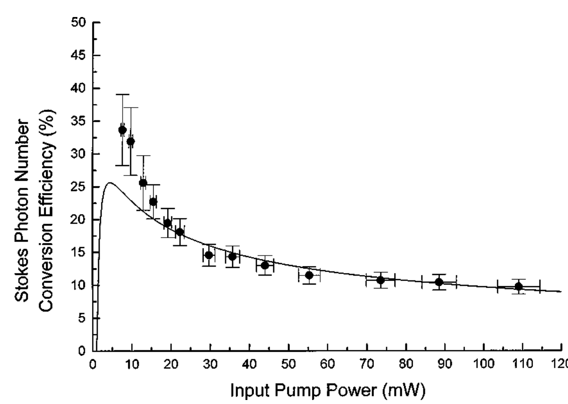

Fig. 8. Plot of the Stokes photon-conversion efficiency at 683 nm as a function of the input pump power at 532 nm. Solid curve, the theoretical predictions; filled circles, experimental measurements. A maximum Stokes photon-conversion efficiency of 34% ± 5.4% is shown.

theoretical prediction. The experiment and theory are in good agreement. A measured threshold for the cw Raman laser is 2 mW.

Figure 8 is a plot of the Stokes photon-conversion efficiency as a function of the input pump power. The filled circles are experimental points, and the solid curve is the theoretical prediction. The maximum Stokes photon-conversion efficiency for this experimental setup is 34% ± 5.4%. Note that mirrors with lower reflectivities would be needed to shift the peak conversion efficiency to higher-input pump powers [see Fig. (5)].

6. RAMAN LASER DESIGN

The depletion factor that gives the maximum Stokes power-conversion efficiency can be found from Eq. (20) as

$$d_{\max} = \frac{TR}{(1 - R^2)} \frac{(1 - R)^2}{(T^2 + AT)}. \qquad (22)$$

With no absorption ($A = 0$), the depletion factor that gives the maximum Stokes power is $d_{\max} = R/(1 + R) = 1/2$ for reflectivities of $R \approx 1$. The maximum Stokes power-conversion efficiency, for $A = 0$, can be found from Eq. (21) with $d = 1/2$ to be $C_S(\max) = {}^1\!/_2(\lambda_p/\lambda_S)$. This

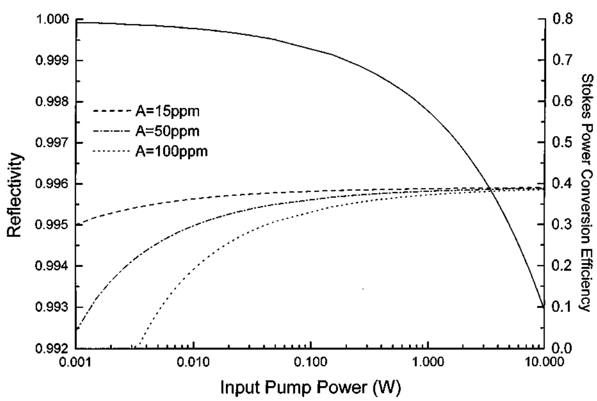

Fig. 9. Solid line curve, plot of the reflectivity that yields the maximum Stokes power-conversion efficiency as a function of the input pump power. The pump (Stokes) wavelength is 532 nm (683 nm). Also the maximum Stokes power-conversion efficiency as a function of the input pump power is shown for absorptions of $A = 15$ ppm (dashed curve), $A = 50$ ppm (dotted–dashed curve), and $A = 100$ ppm (dotted curve).

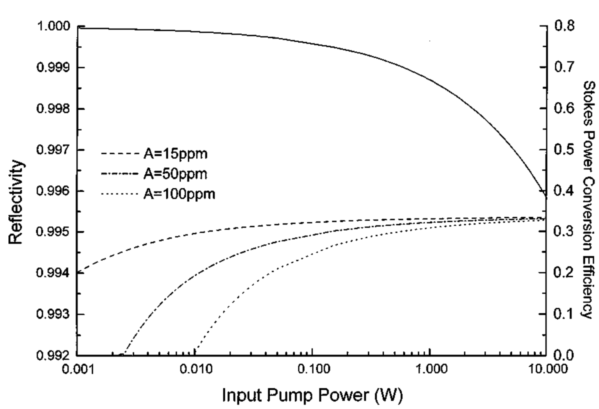

Fig. 10. Same as Fig. 8, except that the pump (Stokes) wavelength is 795 nm (1187 nm).

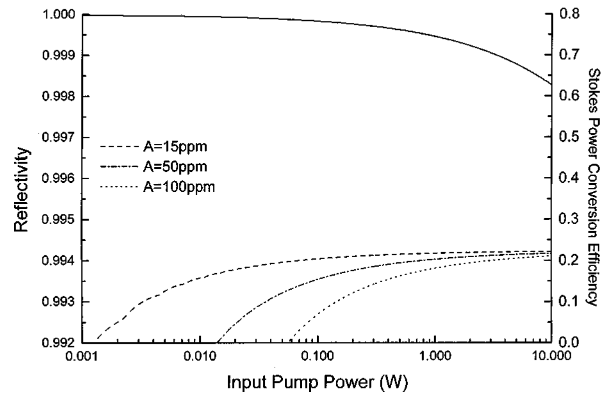

Fig. 11. Same as Fig. 8, except that the pump (Stokes) wavelength is 1330 nm (2973 nm).

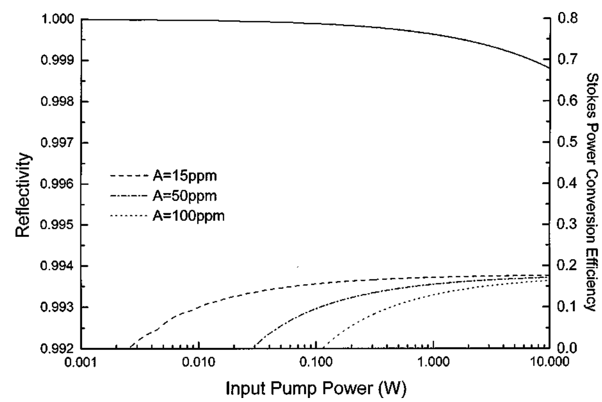

Fig. 12. Same as Fig. 8, except that the pump (Stokes) wavelength is 1550 nm (4350 nm).

sets an upper limit on the conversion efficiency, which will decrease only when absorption of the mirrors is not zero. Finally, the input pump power that gives the maximum conversion efficiency, $P_0(\max)$, can be found from the relationship

$$P_0(\max) = \frac{L_S}{2G_S} \frac{(1 - \sqrt{R})^2}{T} \frac{1}{d_{\max}}. \qquad (23)$$

The design of the Raman laser for maximum conversion efficiency is governed by Eqs. (22) and (23). The input pump power that is governed by the pump laser needs to be matched to the HFC with mirrors at the proper reflectivity and transmission so that Eqs. (22) and (23) are satisfied.

Figure 9 can be used to design a cw Raman laser for a pump laser at 532 nm and a Raman medium of H_2. The input power of the pump laser is assumed to be known. The mirror reflectivity that yields the maximum Stokes power-conversion efficiency is read from the upper curve (solid curve), and the maximum conversion efficiency is then read from the series of three lower curves, depending on the absorption of the mirrors. The dashed curve corresponds to an absorption of 15 ppm, the dotted–dashed curve corresponds to an absorption of 50 ppm, and the dotted curve corresponds to an absorption of 100 ppm. Figures 10–12 are the same as Fig. 9, except the pump lasers have wavelengths of 795 nm, 1330 nm, and 1550 nm, respectively.

7. CONCLUSION

A steady-state theory for the off-resonant cw Raman laser has been presented. This theory predicts a maximum photon-conversion efficiency of 50%. For a 532-nm pump wavelength and a 683-nm Stokes wavelength, the threshold can be as low as 1 mW and the power-conversion efficiency as high as 39%.

The theory was compared with measurements taken with a cw Raman laser that has a pump of 532 nm and a Raman medium of H_2. The cw Raman laser had a measured threshold for the pump power of 2 mW and a maximum Stokes photon-conversion efficiency of 34% $\pm$ 5.4%. The experiment is well modeled by the steady-state theory.

Finally, a simple method for designing cw Raman lasers has been presented. These designs operate near the maximum conversion efficiency and have threshold powers for the pump laser as low as 1 mW. These low threshold values imply that room-temperature diode lasers can be used to pump the cw Raman laser. The Raman-shifted wavelengths of these cw Raman lasers pumped by the available room-temperature diode lasers open up an information-rich spectroscopic region in the mid-infrared part of the spectrum.

ACKNOWLEDGMENTS

This work was supported by a National Science Foundation grant PHY-9424637. K. S. Repasky would also like to acknowledge the many useful discussions with Rand Swanson.

REFERENCES AND NOTES

1. K. S. Repasky, L. E. Watson, and J. L. Carlsten, "High-finesse interferometers," Appl. Opt. **34**, 2615 (1995).
2. K. S. Repasky, J. G. Wessel, and J. L. Carlsten, "Frequency stability of high-finesse interferometers," Appl. Opt. **35**, 609 (1996).
3. E. Hecht, *Optics*, 3rd ed. (Addison-Wesley, New York, 1998).
4. A. Yariv, *Quantum Electronics*, 3rd ed. (Wiley, New York, 1989).
5. N. Bloemberg, "The stimulated Raman effect," Am. J. Phys. **35**, 989 (1967).
6. Y. R. Shen and N. Bloemberg, "Theory of stimulated Brillouin and Raman scattering," Phys. Rev. **137**, 1787 (1965).
7. M. G. Raymer and J. Mostowski, "Stimulated Raman scattering: unified treatment of spontaneous initiation and spatial propagation," Phys. Rev. A **24**, 1980 (1981).
8. P. Rabinowitz, A. Stein, R. Brickman, and A. Kaldor, "Efficient tunable H_2 Raman lasers," Appl. Phys. Lett. **35**, 739 (1979).
9. L. A. Harris and J. N. Lavinos, "Generation of nanosecond infrared pulses tunable from 2.8 to 16 μm by efficient stimulated electronic Raman scattering," Appl. Opt. **26**, 3996 (1987).
10. J. L. Carlsten and R. G. Wenzel, "Stimulated Raman scattering in CO_2-pumped para H_2," IEEE J. Quantum Electron. **QE-19**, 1407 (1983).
11. R. Max, U. Huber, I. Abdul-Halim, J. Heppner, Y. Ni, G. Willenberg, and C. O. Weiss, "Far infrared cw Raman laser gain in $^{14}NH_3$," IEEE J. Quantum Electron. **QE-17**, 1123 (1981).
12. M. Poelker and P. Kumar, "Sodium Raman laser: direct measurement of the narrow-band Raman gain," Opt. Lett. **17**, 399 (1992).
13. S. N. Jabr, "Gain and noise characteristics of a continuous-wave Raman laser," Opt. Lett. **12**, 690 (1987).
14. X. W. Xia, W. J. Sandle, R. J. Ballagh, and D. W. Warrington, "Observation of cw stimulated Raman emission in the neon $2p$-$1s$ manifold," Opt. Commun. **96**, 99 (1993).
15. D. T. Cassidy, "Trace gas detection using 1.3 μm InGaAsP diode laser transmitter modules," Appl. Opt. **27**, 610 (1988).
16. H. I. Schiff, ed., *Measurement of Atmospheric Gases*, Proc. SPIE **1433** (1991).
17. A. Fried, D. K. Killinger, and H. I. Schiff, eds., *Tunable Laser Spectroscopy, Lidar, and Dial Techniques for Environmental and Industrial Measurements*, Proc. SPIE **2112**, (1993).
18. M. Ohtsu, H. Kotani, and H. Tagawa, "Spectral measurements of NH_3 and H_2O for pollutant gas monitoring by 1.5 μm InGaAsP/InP diode lasers," Jpn. J. Appl. Phys., **22**, 1553 (1983).
19. P. Meystre and M. Sargent III, *Elements of Quantum Optics* (Springer-Verlag, New York, 1989); see also R. G. Harrison and Weiping Lu, "Origin of periodic, chaotic, and bistable emission from a Raman laser," Phys. Rev. Lett. **63**, 1372 (1989) for a related theoretical treatment without pump depletion.
20. D. C. MacPherson, R. C. Swanson, and J. L. Carlsten, "Stimulated Raman scattering in the visible in a multipass cell," IEEE J. Quantum Electron. **24**, 1741 (1989).
21. W. K. Bischel and M. J. Dyer, "Wavelength dependence of the absolute Raman gain coefficient for the $Q(1)$ transition in H_2," J. Opt. Soc. Am. B **3**, 677 (1986).
22. J. J. Ottusch and D. A. Rockwell, "Measurement of Raman gain coefficients of hydrogen, deuterium, and methane," IEEE J. Quantum Electron. **24**, 2076 (1989).
23. W. K. Bischel and M. J. Dyer, "Temperature dependence of the Raman linewidth and line shift for the Q(0) and Q(1) transition in normal and para H_2," Phys. Rev. A **33**, 3113 (1986).
24. The mirrors used for the cw Raman laser were purchased from Research ElectroOptics Inc., 1855 South 57th Court, Boulder, Colo., 80301.
25. J. K. Brasseur, K. S. Repasky, and J. L. Carlsten, "Continuous-wave Raman laser in H_2," Opt. Lett. **23**, 367 (1998).